EURASIAN JOURNAL OF MATHEMATICAL AND COMPUTER APPLICATIONS
ISSN 2306–6172
Volume 12, Issue 4 (2024) 4 – 11

DIRECT NUMERICAL SIMULATION OF TWO-COMPONENT SWIRLING JET ATOMIZATION

Apostol Yu.S., Vozhakov I.S., Hrebtov M.Yu., Mullyadzhanov R.I.

Abstract The direct numerical study of two immiscible liquids atomization with a centrifugal nozzle was carried out at different flow rates The simulation was performed in the Basilisk package and was carried out in 2 stages. At the first stage, the flow inside the nozzle was simulated. As a result, the profiles of the liquid content and the three components of the velocity at the nozzle exit were obtained. Then, these data were used to simulate the spray of the jet in the external half-space. Characteristic patterns of the outflow of the two-component jet and the distribution of droplets by size, depending on the liquid flow rates, were obtained.

Key words: immiscible liquids, spray formation, droplets, centrifugal nozzle.

AMS Mathematics Subject Classification: 76M12.

DOI: 10.32523/2306-6172-2024-12-4-4-11

1 Introduction

The processes of interaction between two immiscible liquids are widespread in various industries, including the production of paints and varnishes, cosmetics, pharmaceuticals, as well as in the spraying of liquid fuels. Among the main problems of using liquid fuel is environmentally efficient combustion [1, 2, 3]. The solution of environmental problems is often associated with the addition of special impurities to the fuel composition [4, 5, 6]. In recent years, technological solutions with the addition of water to the fuel composition have become increasingly popular [7, 8, 9].

The main physical mechanism for reducing the concentration of harmful sulfur and nitrogen oxides is their interaction with the resulting water vapor. The calorific value of such fuel suspensions and emulsions is lower than that of pure fuels. However, when a significant reduction in anthropogenic emissions is required, the addition of water to the fuel is one of the most rational solutions.

The addition of water can also be used to intensify the heating, evaporation, and ignition of fuel droplets [10, 11, 12]. At first glance, this approach seems contradictory, since additional energy is spent on the evaporation of water. However, a significant advantage arises due to the processes of explosive disintegration of fuel droplets when water is added to their composition [13, 14, 15].

Despite significant progress in modeling two-phase flows, the task of numerical simulation of the dynamics of spraying two immiscible liquids remains complex and insufficiently studied. Due to the lower practical application of such flows at the moment, as well as due to the difficulties arising from the passage of two interfaces through the

volume of the computational cell, only a small number of works consider the modeling of processes in jets of immiscible liquids [16, 17, 18, 19]. The key aspect in the spraying of immiscible liquids is the dynamics of their motion inside the centrifugal nozzle and during the outflow from it. The nature of the outflow and the dispersion of the resulting droplets depend on a wide range of factors, including the geometry of the nozzle, the physical properties of the liquids, and the outflow modes. Particular difficulties are posed by the interfacial interaction processes, pressure pulsations, as well as phenomena associated with the unsteadiness of the flow and the deformation of the free surface. In addition, colossal computing power is required to resolve the flow in detail, both inside the nozzle and in the external region.

The presented work proposes a comprehensive mathematical model that allows the numerical investigation of the dynamics of spraying two immiscible liquids from a centrifugal nozzle. The model is based on the solution of the Navier-Stokes equation system, taking into account the interphase interaction and the deformation of the free surface. The calculations are carried out in two stages. At the first stage, the flow inside the nozzle is simulated. This makes it possible to obtain the spatial-temporal profiles of velocity and volume fraction of liquids at the nozzle exit. These profiles are then used to calculate the outflow of the two-component jet into the external space. This approach allows a significant reduction in the computational power and calculation time used. In this work, the open-source Basilisk computational code was used. This code is specialized for calculating flows with an interphase surface and has been validated for various flows [20, 21, 22]. In particular, a detailed comparison with an experiment for two immiscible liquids in a gas atmosphere was carried out in [22], and the simulation of the spray of a single-component jet was performed in [23]. The comparison showed good agreement between the calculated data and the experiment. Based on the results of numerical modeling, an analysis of the patterns of formation of a two-phase jet flow and the operating parameters on the spray characteristics was performed.

The results of the study contribute to understanding the mechanisms of formation of two-phase jets when using centrifugal nozzles and can be used to optimize the design and operating modes of such systems in various technological applications.

2 Numerical procedure

2.1 Governing equations

The modeling is based on the numerical solution of the Navier-Stokes equations for an incompressible fluid:

$$\frac{\partial u_i}{\partial x_i} = 0, \qquad \frac{\partial u_i}{\partial t} + \frac{\partial u_i u_j}{\partial x_j} = -\frac{1}{\rho}\frac{\partial p}{\partial x_i} + \frac{\partial \tau_{ij}}{\partial x_j} + \frac{f_{\sigma,i}}{\rho}$$

where u_i, x_i are the velocity components and coordinates, p is the pressure field, ρ is the density, $\tau_{i,j} = \nu(\frac{\partial u_i}{\partial x_j} + \frac{\partial u_j}{\partial x_i})$ represents the viscous tensor, ν is the kinematic viscosity. The surface tension force is defined as $f_{\sigma,i} = (\sigma_1\kappa_1 n_{1,i} + \sigma_2\kappa_2 n_{2,i} + \sigma_3\kappa_3 n_{3,i})\delta_s$, where $\kappa_m = -\nabla n_m$ is the surface curvature, $n_m = \frac{\nabla\alpha_m}{|\nabla\alpha_m|}$ is the normal vector to the surface,

σ_m is the surface tension coefficient. The Dirac delta function δ_s is not zero only at the interface.

Multi-phase calculations require the use of free surface tracking models, in this case, the volume of fluid method is used, which is governed by the equations:

$$\frac{\partial \alpha_m}{\partial t} + u_i \frac{\partial \alpha_m}{\partial x_i} = 0 \qquad m = 1, 2,$$

where α_m is the volume fraction of the m-th phase. Thus, the local characteristics (density and dynamic viscosity) are determined as:

$$\rho = \alpha_1 \rho_1 + \alpha_2 \rho_2 + (1 - \alpha_1 - \alpha_2)\rho_3, \qquad \mu = \alpha_1 \mu_1 + \alpha_2 \mu_2 + (1 - \alpha_1 - \alpha_2)\mu_3.$$

2.2 Computational domain

The simulation was carried out in a cubic domain, including a nozzle (Fig. 1) with two supply channels with diameters of 1.2 mm and an outlet nozzle diameter D_0 of 0.8 mm.

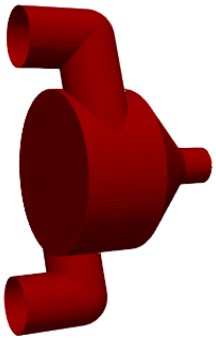

Figure 1: The centrifugal nozzle.

The fluids used are water with a density of $\rho_1 = 1000$ kg/m^3 and a dynamic viscosity of $\mu_1 = 10^{-3}$ kg/m $\cdot\, s$ and kerosene with $\rho_2 = 800\ kg/m^3$ and $\mu_2 = 1.5 \cdot 10^{-3}\ kg/m\,s$. In the calculations, the inlet velocity in the supply channels U_0 was 4, 5 and 6 m/s. The corresponding Reynolds numbers Re are 8000, 12000 and 14400.

The computational procedure used the adaptive grid refinement method, with the smallest cell size Δ_{min} being 2 μm. The Kolmogorov length scale η, estimated at the nozzle exit, was 1 μm.

In the simulation of the internal flow, a constant normal velocity u_n was specified as the boundary condition in the supply channels, while the other components (u_t, u_r) were set to zero: $u_n = U_0, \quad u_t = 0, \quad u_r = 0, \quad \nabla p = 0$

On the nozzle walls, the conditions of no-slip and no-flow were specified:

$$u_n = 0, \quad u_t = 0, \quad u_r = 0, \quad \nabla p = 0$$

At the nozzle exit, free outflow conditions were specified:

$$\nabla u = 0, \quad \nabla p = 0 \tag{1}$$

In the simulation of the jet spray in the external space, the jet velocity was read from previously recorded files. On the other remaining boundaries, the free outflow condition (1) was specified. In the simulation of the flow in the internal and external spaces, the condition of the average pressure being equal to zero was also used.

3 Results

The simulation was carried out in two stages: at the first stage, the flow inside the nozzle was calculated. As a result, the fields of velocity, phases and pressures at the nozzle exit were obtained, which were then transmitted as boundary conditions for the second stage of the calculation. This approach made it possible to significantly increase the resolution of the computational grid and reduce the calculation time.

3.1. The flow inside the nozzle

At this stage, the simulation of the internal flow inside the centrifugal nozzle was carried out. At the initial time, the nozzle was equally filled with stationary liquids with an interface passing through the center of the nozzle. After the start of the calculation, the liquid flows from the inlet channels lead to the swirling of the liquids inside the nozzle. At the same time, the initial planar interface breaks up with the formation of droplets of both liquids.

About 1 ms after the start of the calculation, the jet at the nozzle exit flows out with a nonzero tangential velocity component. Starting from this moment in time and over the next 5 ms, the velocity components in the output section were recorded. After that, they were averaged over time. As a result, the velocity distributions presented in Figure 2 were obtained. After angular averaging, the velocity profiles close to the known dependencies for centrifugal nozzles were obtained. Fig. 3 shows the obtained dependencies of the axial and tangential velocity components. At the same time, as expected, the tangential velocity is an order of magnitude lower than the axial velocity, but its value increases with an increase in the liquid flow rate. The radial velocity component turns out to be 2 orders of magnitude smaller than the axial component.

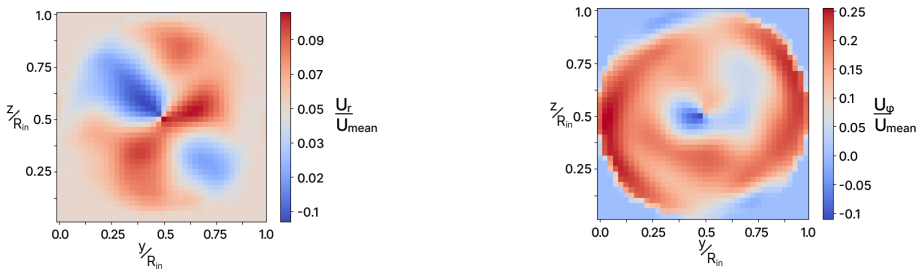

Figure 2: The field of the radial and tangential velocity components at the nozzle exit.

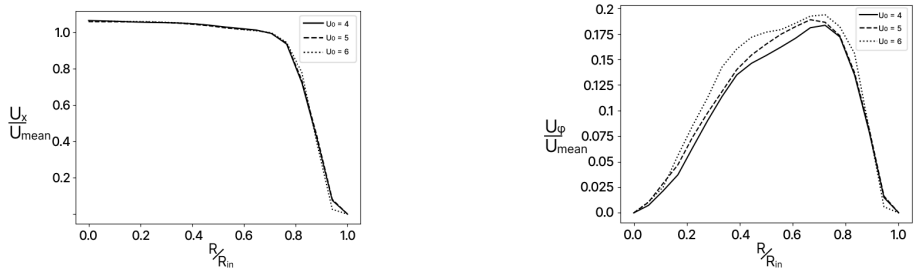

Figure 3: Radius-averaged axial and tangential velocity components at the nozzle exit.

3.2. Spray in the external space

At the second stage, the simulation of the jet outflow from the nozzle into the external atmosphere was carried out using the instantaneous velocity distributions obtained earlier. This approach allows not only preserving the natural characteristics of turbulence, but also making the computational grid more detailed without increasing the calculation time. During the outflow, the jet takes the form of a hollow cone, the walls of which deform as they move away from the nozzle. In the single-liquid case (Fig. 4a),

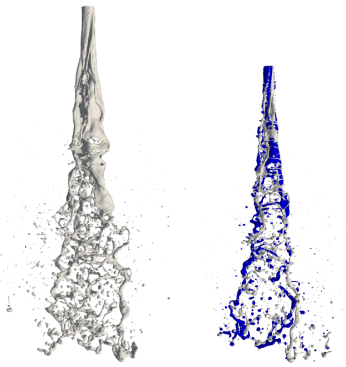

Figure 4: The flowing jet. U_0=5 m/s. Water is marked in blue, kerosene in white.

perforation is observed in the walls of the cone, caused by the Kelvin-Helmholtz instability. Then these instabilities continue to grow, which leads to the formation of ligaments (elongated ligatures), and then to the formation of liquid droplets.

In the two-liquid case (Fig. 4b), as mentioned above, droplet inclusions appear already at the stage of internal flow in the nozzle. Therefore, when flowing out into the external atmosphere, the jet breakup occurs much faster. The presence of an additional interface surface within the jet leads to a faster growth of disturbances.

Upon reaching the quasi-stationary outflow, i.e. when the jet reaches the boundaries of the computational domain (we assume that the velocity at the nozzle exit has stabilized), data collection on the volume and coordinates of the drops begins every 0.1 ms. For this, an algorithm is used that counts the number of connected regions where the liquid content α_m is equal to one. Then, the radius of the detected droplets is calculated from the measured volume, assuming that all droplets are spherical. Based on these data, for each time point, histograms of the dependence of the number of droplets on their radius with a cell width of 1 μm are constructed. After that, the obtained droplet distributions are averaged over time as arithmetic means. Fig. 5 shows the histograms of the droplet size distribution, averaged over 5 ms of calculation. It is shown that in the two-liquid case, the peak of the kerosene droplet distribution shifts to the left compared to the single-liquid case. At the same time, in the two-liquid case, the number of kerosene droplets relative to the total kerosene outflow volume is higher. Thus, it can be argued that the two-component jet breaks up into a larger number of smaller droplets compared to the single-component jet.

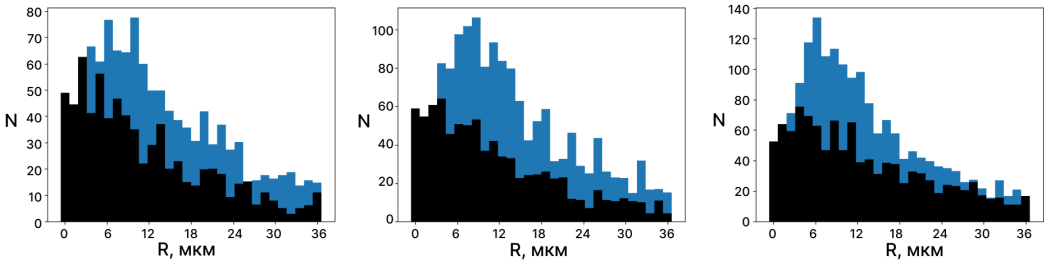

Figure 5: Distribution of the number of kerosene droplets by size. Blue color - single-liquid, black - two-liquid case. a) U_0=4 m/s, b) U_0=5 m/s, c) U_0=6 m/s.

4 Conclusion

Numerical modeling of the flow of two immiscible liquids from a centrifugal nozzle at various flow regimes was carried out in this study. The modeling was performed in two stages: first, the flow inside the nozzle was investigated, and then the spray of the jet into the external space was studied.

The results showed that in the single-liquid case, perforation is observed on the walls of the cone of the jet, caused by the Kelvin-Helmholtz instability. These instabilities continue to develop, leading to the formation of ligaments and the subsequent breakup of the jet into droplets.

In the two-liquid case, the breakup occurs much faster due to the presence of an additional interfacial surface within the jet, which promotes faster growth of disturbances. Thus, the introduction of the second liquid significantly changes the nature of the jet breakup. The kerosene droplets formed during the atomization in the two-liquid case are smaller, and their number increases.

Acknowledgement

The work was carried out with the support of the Russian Science Foundation (grant No. 22-79-10246).

References

[1] Kontorovich A.E., Epov M.I., Eder L.V., *Long-term and medium-term scenarios and factors in world energy perspectives for the 21st century*, Russ. Geol. Geophys., 55 (2014), 534–543

[2] Lior N., *Energy resources and use: the present situation and possible paths to the future*, Energy, 33 (2015), 842-857.

[3] Glushkov D.O., Strizhak P.A., Chernetskii M.Yu., *Organic coal-water fuel: problems and advances (review)*, Therm. Eng., 10 (2016), 707-717.

[4] Fitzpatrick E.M., Bartle K.D., Kubacki M.L., Jones J.M., Pourkashanian M., Ross A.B., Williams A., Kubica K., *The mechanism of the formation of soot and other pollutants during the co-firing of coal and pine wood in a fixed bed combustor*, Fuel, 88 (2009), 2409-2417.

[5] Shahzad K., Saleem M., Kazmi M., Ali J., Zulfiqar, Hussain S., Akhtar, N.A., *Effect of hydrodynamic conditions on emissions of NOx, SO2, and CO from co-combustion of wheat straw and coal under fast fluidized bed condition*, Combust. Sci. Technol., 188 (2016), 1303-1318.

[6] Lee B.-H., Lkhagvadorj Sh., Bae J.-S., Choi Y.-Ch., Jeon Ch.-H., *Combustion behavior of low-rank coal impregnated with glycerol*, Biomass Bioenergy, 87 (2016), 122-130.

[7] Kichatov B., Korshunov A., Son K., Son E., *Combustion of emulsion-based foam*, Combust. Flame, 172 (2016), 162-172.

[8] Kichatov B., Korshunov A., Kiverin A., Son E., *Foamed emulsion — fuel on the base of water-saturated oils*, Fuel, 203 (2017), 261-268.

[9] Antonov D. V., Volkov R. S., Strizhak P. A., *An explosive disintegration of heated fuel droplets with adding water*, Chemical Engineering Research and Design, 140 (2018), 292-307.

[10] Mitre J., Lage P., Souza M., Silva E., Barca L., Moraes A., Coutinho R., Fronseca E., *Droplet breakage and coalescence models for the flow of water-in-oil emulsions through a valve-like element*, Chem. Eng. Res. Des., 92 (2014), 2493-2508.

[11] Shao T., Bai L., Yan B., Jin Y., Cheng Y., *Modeling the solidification of O/W-emulsion droplet in solvent evaporation technique*, Chem. Eng. Res. Des., 122 (2017), 233-242.

[12] Yue S., Mansouri S., Woo M., Chen X., 2013. *Antisolvent vapour precipitation of droplets with multi-components: non-soluble encapsulation and simultaneous precipitation of soluble materials*, Chem. Eng. Res. Des., 91 (2013), 1705-1714.

[13] Suzuki Y., Harada T., Watanabe H., Shoji M., Matsushita Y., Aoki H., Miura T., *Visualization of aggregation process of dispersed water droplets and the effect of aggregation on secondary atomization of emulsified fuel droplets*, Proc. Combust. Inst., 33 (2011), 2063-2070.

[14] Tarlet D., Josset C., Bellettre J., *Comparison between unique and coalesced water drops in micro-explosions scanned by differential calorimetry*, Int. J. Heat Mass Transf., 95 (2016), 689-692.

[15] Antonov D. V., Kuznetsov G. V., Voytkov I. S., Strizhak P. A., Volkov R. S., *Cascade fragmentation of composite parent and child droplets*, Fuel, 333 (2023), 126522.

[16] Tsuru D., Tajima H., Ishibashi R., Kawauchi S., *Droplet collision modelling between merging immiscible sprays in direct water injection system*, In ILASS Europe, 23rd annual conference on liquid atomization and spray systems (2010), Brno, Czech Republic.

[17] Potyka J., Schulte K., *A volume of fluid method for three dimensional direct numerical simulations of immiscible droplet collisions*, International Journal of Multiphase Flow, 170 (2024), 104654.

[18] Chen X., Ma D., Yang V., *Mechanism study of impact wave in impinging jets atomization*, 50th AIAA Aerospace Sciences Meeting including the New Horizons Forum and Aerospace Exposition (2012), 1089.

[19] Vozhakov I., Hrebtov M., Mullyadzhanov R., *Numerical simulation of a two-component jet atomization*, E3S Web of Conferences, 459 (2023), 04004.

[20] Salvador F. J., Martí-Aldaraví P., Lozano A., Taghavifar H., Nemati A., *Droplet characterization of a pressure-swirl atomizer by means of high-fidelity modelling based on DNS simulations*, Fuel, 358 (2024), 130169.

[21] Hashemi M., Shalbaf S., Jadidi M., Dolatabadi A., *Effects of gas viscosity and liquid-to-gas density ratio on liquid jet atomization in crossflow*, AIP Advances, 13(2023).

[22] Fudge B. D., Cimpeanu R., Castrejón-Pita A. A., *Drop impact onto immiscible liquid films floating on pools*, Scientific Reports, 14(2024), 13671.

[23] Vozhakov I. S., Hrebtov M. Y., Yavorsky N. I., Mullyadzhanov R. I., *Numerical Simulations of Swirling Water Jet Atomization: A Mesh Convergence Study*, Water, 15(2023), 2552.

Yulia S. Apostol,
Kutateladze Institute of Thermophysics SB RAS,
Russia, Novosibirsk, Lavrentieva av, 1
Email: y.apostol@g.nsu.ru

Ivan S. Vozhakov,
Kutateladze Institute of Thermophysics SB RAS,
Russia, Novosibirsk, Lavrentieva av, 1
Email: vozhakov@gmail.com

Michael Yu. Hrebtov,
Kutateladze Institute of Thermophysics SB RAS,
Russia, Novosibirsk, Lavrentieva av, 1
Email: weexov@ya.ru

Rustam I. Mullyadzhanov,
Kutateladze Institute of Thermophysics SB RAS,
Russia, Novosibirsk, Lavrentieva av, 1
Email: rustammul@gmail.com

Received 10.08.2024 Accepted 02.10.2024